

Electronic Supplementary Information for:

Phase stabilization of red-emitting olivine-type $\text{NaMgPO}_4:\text{Eu}^{2+}$ phosphors via molten-phase quenching

Takuya Hasegawa,^{1*} Masato Iwaki,² Ryo Tanaka,² Sun-woog Kim,^{2,3*} Shu Yin,¹ Kenji Toda^{2*}

¹*Institute of Multidisciplinary Research for Advanced Material (IMRAM), Tohoku University, 2-1-1 Katahira, Aoba-ku, Sendai, 980-8577, Japan*

²*Graduate School of Science and Technology, Niigata University, 8050 Ikarashi 2-nocho, Niigata 950-2181, Japan*

³*Electronic Convergence Materials Division, Optic and Display Materials Center, Korea Institute of Ceramic Engineering and Technology, 101 Soho-ro, Jinju-si, Republic of Korea*

Keywords: *Eu^{2+} -doped phosphor, Red emission, phosphor, pc-WLED, Phase stabilization, Molten-phase quenching process*

*Corresponding authors

Assistant Professor Dr. Takuya Hasegawa

Tel +81-22-217-5599, E-mail: hase@tohoku.ac.jp

Dr. Sun-woog Kim

Tel +82-55-792-2487, E-mail: skim80@kicet.re.kr

Research Professor Dr. Kenji Toda

Tel/Fax +81-25-262-6771, E-mail: ktoda@eng.niigata-u.ac.jp

Content

1. Figure S1 Results of the Rietveld analysis of the $\text{NMP:}_{0.025}\text{Eu}$ -arc phosphor.
2. Table S1 Details of the Rietveld refinement of the olivine-type $\text{NMP:}_{0.025}\text{Eu}$ -arc phosphor.
3. Figure S2 Schematic illustration of the experimental procedure for the humidity resistance test.
4. Figure S3 (left) XRD patterns of the $\text{NMP:}_{0.030}\text{Eu}^{2+}$ phosphors synthesized by the conventional solid-state reaction method *via* a normal cooling process using alumina and carbon boats and *via* a molten-phase quenching route using an alumina boat. (right) Photographs of these phosphors irradiated by 365 nm black light.
5. Figure S4 (A) TG and (B) all-range DTA curves measured under the same conditions as in Figure 1A for the preheated precursor of the $\text{NMP:}_{0.030}\text{Eu}^{2+}$ phosphor.
6. Table S2 Details of the Rietveld refinement of the olivine type $\text{NMP:}_x\text{Eu}^{2+}\text{-MPQ}$ ($x=0\text{-}0.100$) phosphors.
7. Figure S5 Lattice constants, (A) a , (B) b and (C) c , and (D) volume of the olivine-type $\text{NMP:}_x\text{Eu}^{2+}\text{-MPQ}$ ($x=0\text{-}0.100$) phosphors.
8. Figure S6 Dependence of the BVS values of the Na (4a) and Mg (4c) sites on the Eu^{2+} concentration in the olivine-type $\text{NMP:Eu}^{2+}\text{-MPQ}$ phosphor.
9. Table S3 Mean bond length of the $\text{NMP:}_{0.030}\text{Eu}$ -MPQ phosphor.
10. Figure S7 XPS spectra for (a) $\text{NMP:}_{0.030}\text{Eu}^{2+}\text{-MPQ}$ and (b) $\text{NMP:Eu}_{0.025}\text{-arc}$ phosphors: survey, Na1s, Mg2p, P2p and O1s.
11. Table S4 Chemical analysis based on the XPS results for the $\text{NMP:}_{0.030}\text{Eu}^{2+}\text{-MPQ}$ and $\text{NMP:}_{0.025}\text{Eu}$ -arc phosphors.
12. Figure S8 FE-SEM image of the olivine-type $\text{NMP:}_{0.025}\text{Eu}$ -arc phosphor.
13. Figure S9 Plot of the Kubelka-Munk function for the NMP host.
14. Figure S10 Photographs of the non-excited $\text{NMP:}_x\text{Eu}^{2+}\text{-MPQ}$ ($x=0.010\text{-}0.050$) and $\text{NMP:}_{0.025}\text{Eu}$ -arc phosphors (under fluorescent lamps).
15. Figure S11 (A) PL and PLE spectra and (B) plot of the PL intensity for $\text{NMP:}_x\text{Eu}^{2+}\text{-MPQ}$ ($x=0.010\text{-}0.050$) phosphors.
16. Figure S12 PL decay curves for the $\text{NMP:}_{0.030}\text{Eu}^{2+}\text{-MPQ}$ phosphors before and after the humidity test.

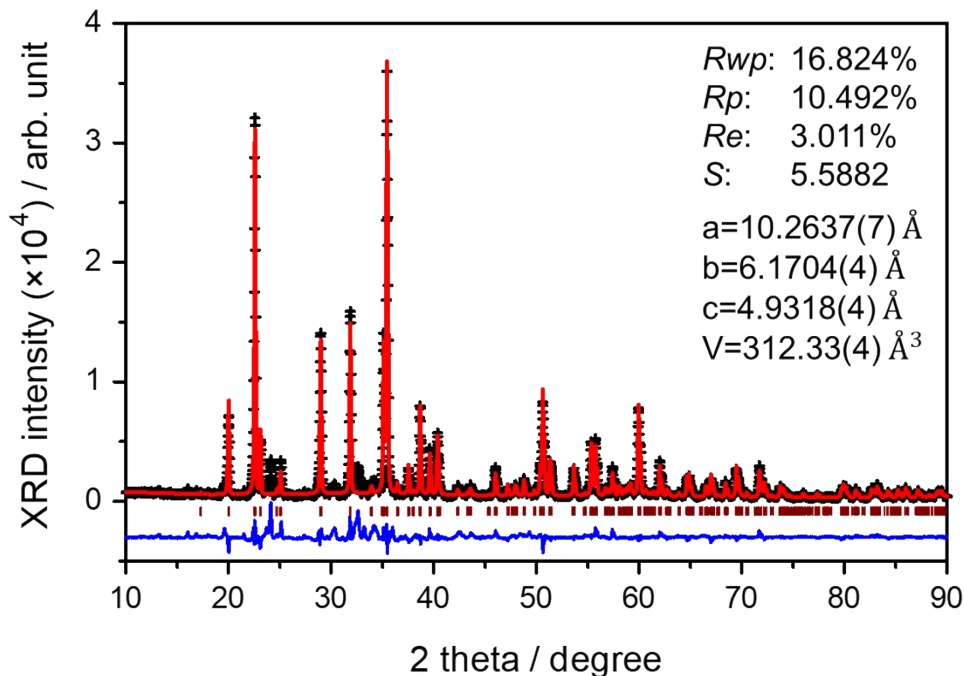


Figure S1 Results of the Rietveld analysis of the NMP:_{0.025}Eu-arc phosphor.

Table S1 Details of the Rietveld refinement of the olivine-type NMP:_{0.025}Eu-arc phosphor.

Atom	Wyckoff	Occ. ^a	x	y	z	U_{iso} . ^b (Å ²)	BVS ^c
Na1/Eu1	4a	1	0	0	0	0.5(1)	1.41(6)
Mg1	4c	1	0.2820(4)	0.25	0.9933(9)	0.1(1)	1.83(6)
P1	4c	1	0.1093(4)	0.25	0.4439(7)	0.3(1)	4.9(1)
O1	4c	1	0.1202(8)	0.25	0.750(1)	0.407	2.2(2)
O2	4c	1	0.4642(8)	0.25	0.154(1)	0.4(2)	2.20(4)
O3	8d	1	0.1747(6)	0.0542(7)	0.3039(10)	0.6(2)	2.14(4)

^a Occ. means atomic occupancy; ^b isotropic temperature factors; ^c bond valence sum

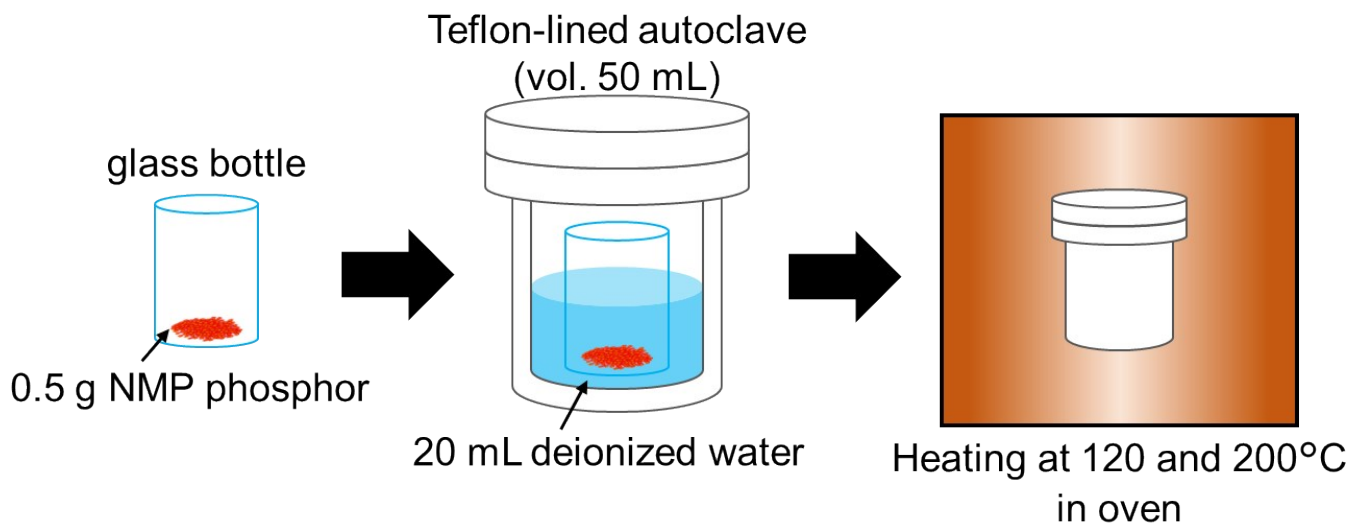


Figure S2 Schematic illustration of the experimental procedure for the humidity resistance test.

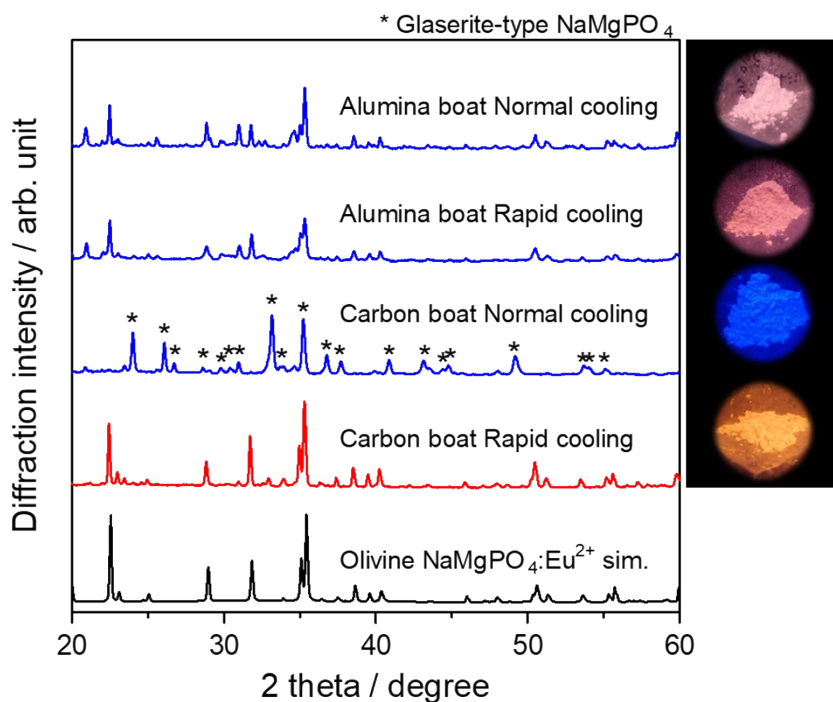


Figure S3 (left) XRD patterns of the $\text{NMP:}_{0.030}\text{Eu}^{2+}$ phosphors synthesized by the conventional solid-state reaction method *via* a normal cooling process using alumina and carbon boats and *via* a molten-phase quenching route using an alumina boat. (right) Photographs of these phosphors irradiated by 365 nm black light.

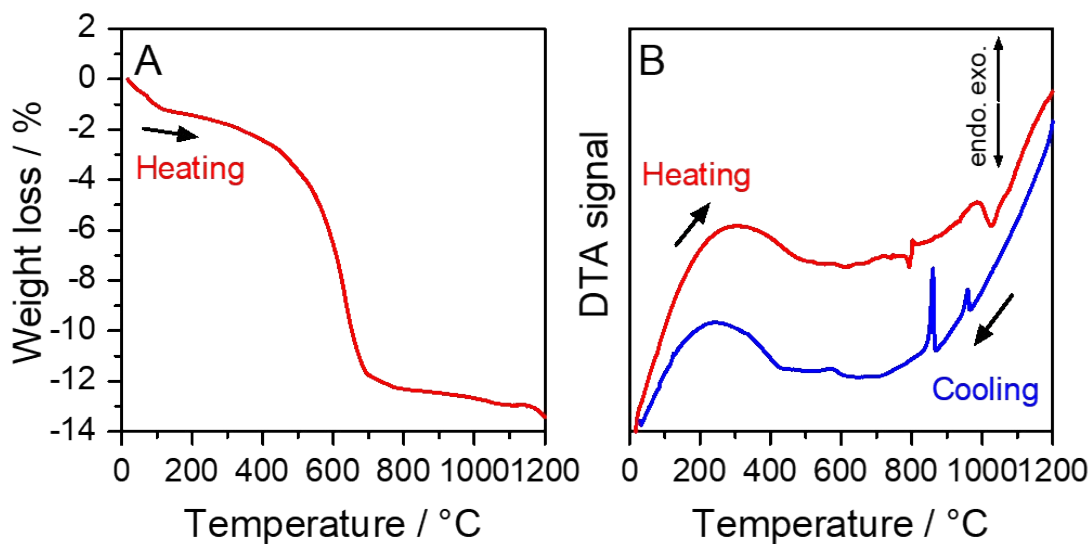


Figure S4 (A) TG and (B) all-range DTA curves measured under the same conditions as in Figure 1A for the preheated precursor of the NMP:Eu²⁺ phosphor.

Table S2 Details of the Rietveld refinement of the olivine-type NMP;_xEu²⁺-MPQ (x=0-0.100) phosphors.

x	R_{wp} (%)	R_p (%)	R_e (%)	S
0	17.419	10.874	3.679	4.7343
0.01	11.311	7.848	3.492	3.2388
0.02	10.918	7.314	3.406	3.2057
0.025	10.675	6.826	3.333	3.2024
0.03	10.212	6.247	3.225	3.1666
0.04	10.377	6.353	3.086	3.3625
0.05	13.104	8.123	3.027	4.3285
0.06	14.381	8.966	2.927	4.9136
0.08	15.285	8.84	2.831	5.3984
0.1	15.205	9.253	2.739	5.5503

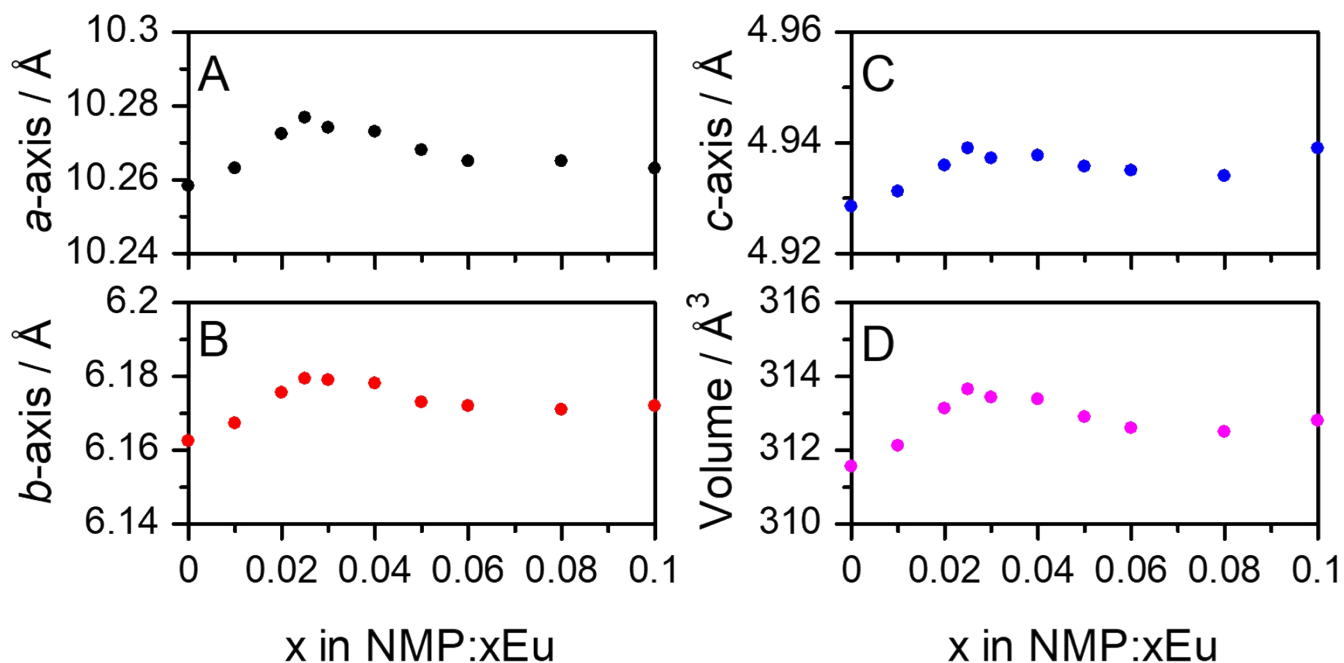


Figure S5 Lattice constants, (A) a , (B) b and (C) c , and (D) volume of the olivine-type NMP: x Eu²⁺-MPQ ($x=0-0.100$) phosphors.

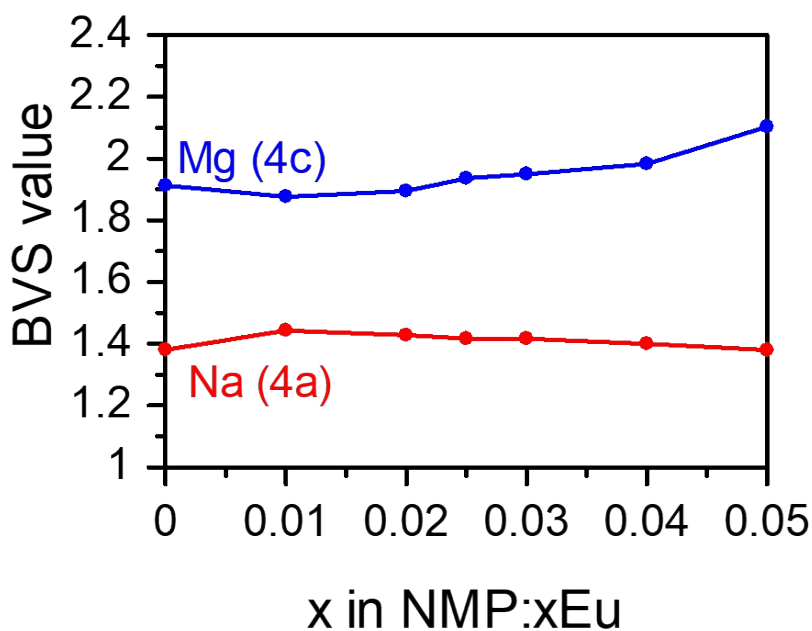


Figure S6 Dependence of the BVS values of the Na (4a) and Mg (4c) sites on the Eu²⁺ concentration in the olivine-type NMP:Eu²⁺-MPQ phosphor.

Table S3 Mean bond length of the NMP:_{0.030}Eu-MPQ phosphor.

Cation	Anion	Bond length (Å)
Na1	O1×2	2.341(6)
	O2×2	2.332(5)
	O3×2	2.371(5)
Average		2.348
Mg1	O1	2.026(9)
	O2	2.003(9)
	O3×2	2.238(6)
	O3×2	2.150(5)
Average		2.134
P1	O1	1.544(7)
	O2	1.593(9)
	O3×2	1.535(5)
Average		1.552

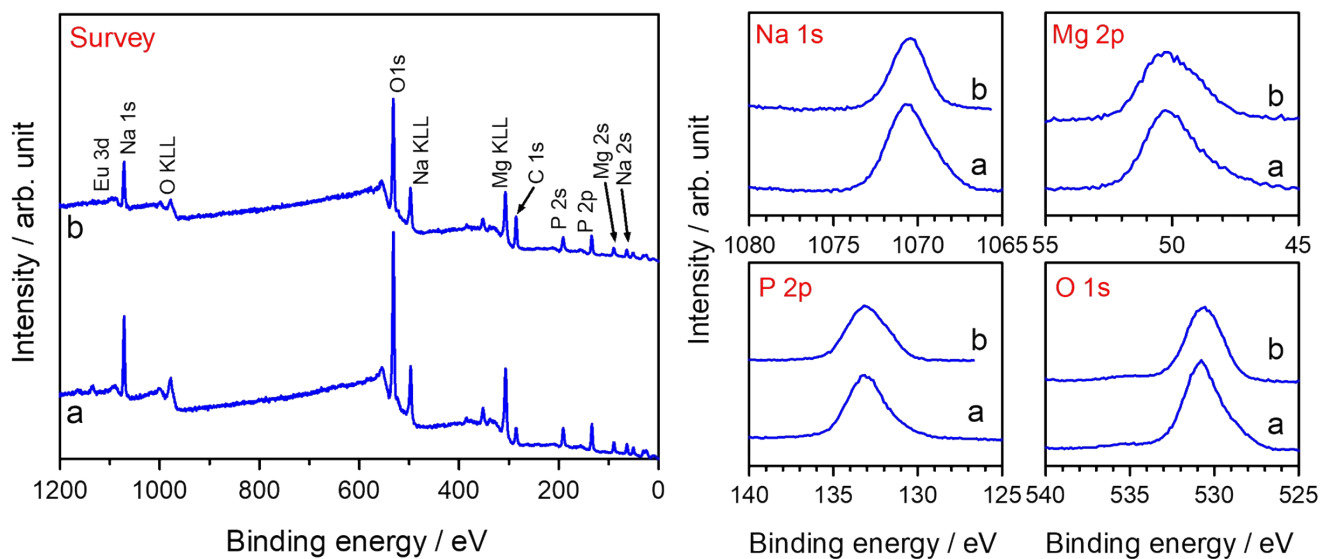
**Figure S7** XPS spectra for (a) NMP:_{0.030}Eu²⁺-MPQ and (b) NMP:Eu_{0.025}-arc phosphors: survey, Na1s, Mg2p, P2p and O1s.

Table S4 Chemical analysis based on the XPS results for the NMP:_{0.030}Eu²⁺-MPQ and NMP:_{0.025}Eu-arc phosphors.

Elements	Level	Atomic concentration (%)	
		NMP: _{0.030} Eu-MPQ	NMP: _{0.025} Eu-arc
Na	1s	18.89	15.74
Eu	3d	0.55	0.30
Mg	2p	13.59	14.76
P	2p	14.83	16.55
O	1s	52.14	52.65

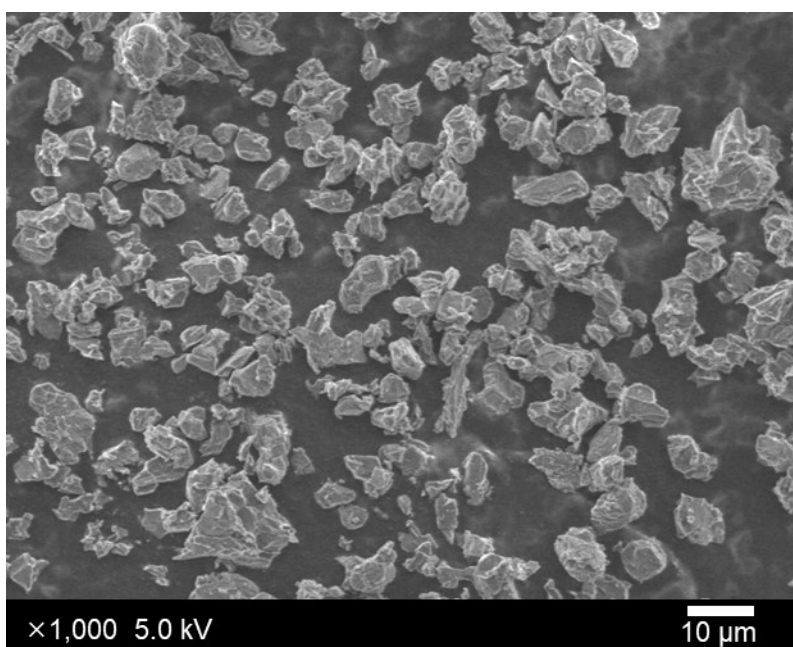


Figure S8 FE-SEM image of the olivine-type NMP:_{0.025}Eu-arc phosphor.

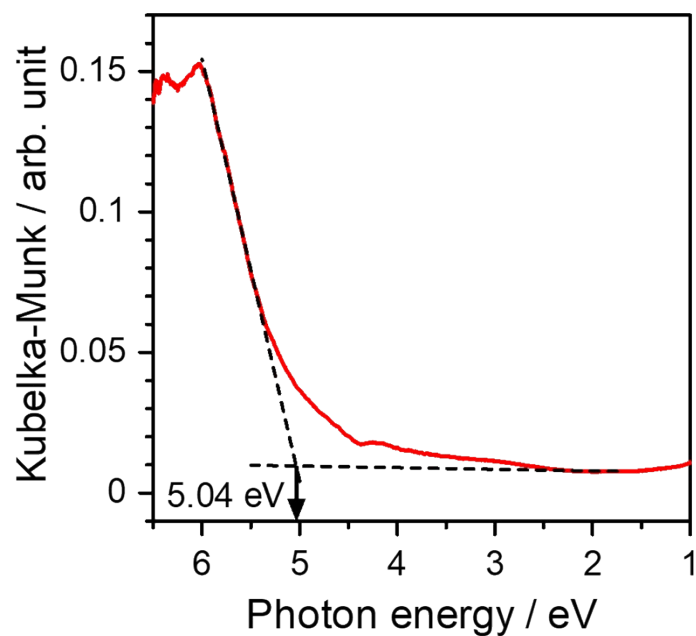


Figure S9 Plot of the Kubelka-Munk function for the NMP host.

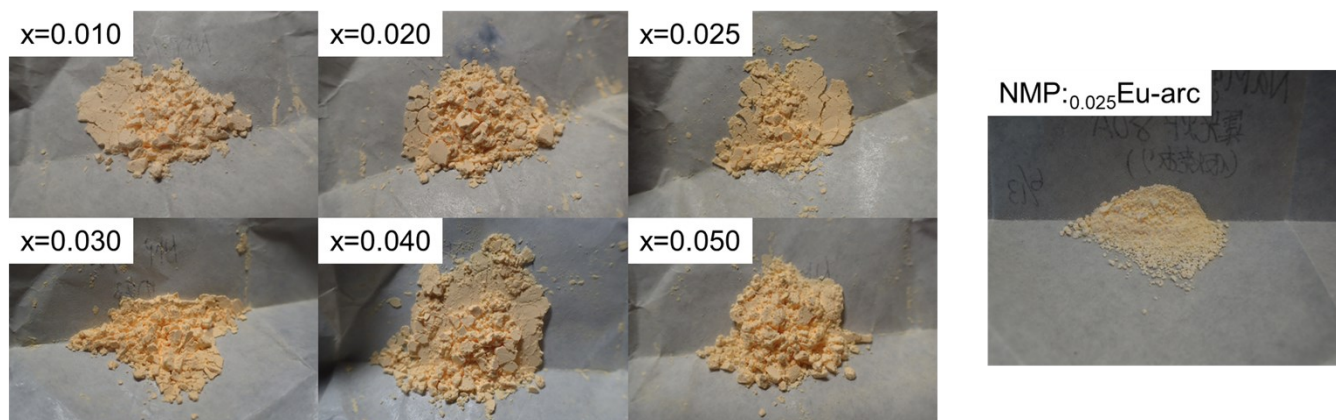


Figure S10 Photographs of the non-excited $\text{NMP}:_x\text{Eu}^{2+}\text{-MPQ}$ ($x=0.010\text{-}0.050$) and $\text{NMP}:_{0.025}\text{Eu-arc}$ phosphors (under fluorescent lamps).

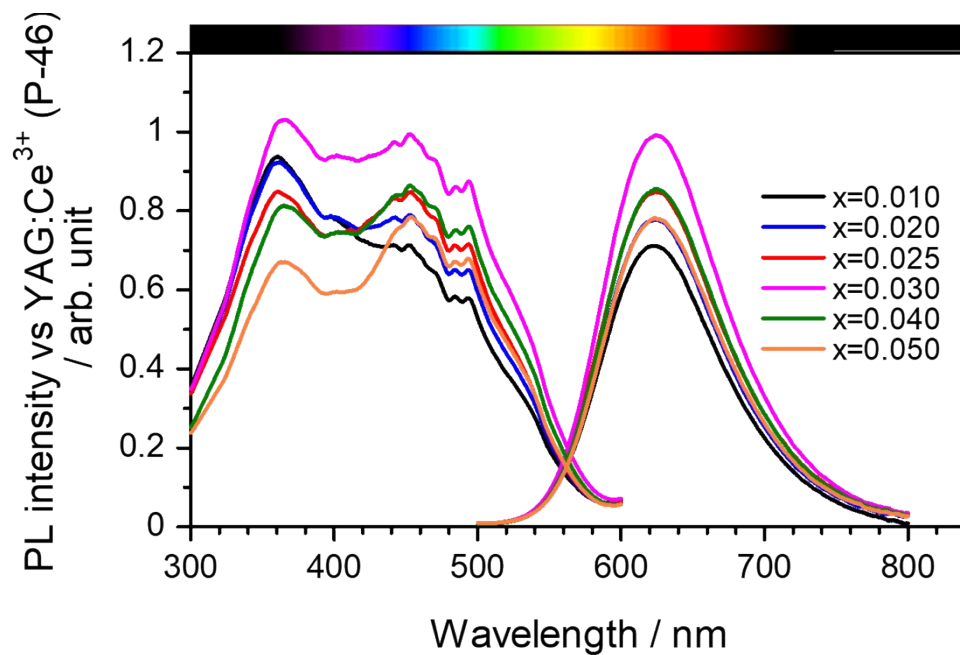


Figure S11 (A) PL and PLE spectra and (B) plot of the PL intensity for the NMP: x Eu²⁺-MPQ ($x=0.010$ - 0.050) phosphors.

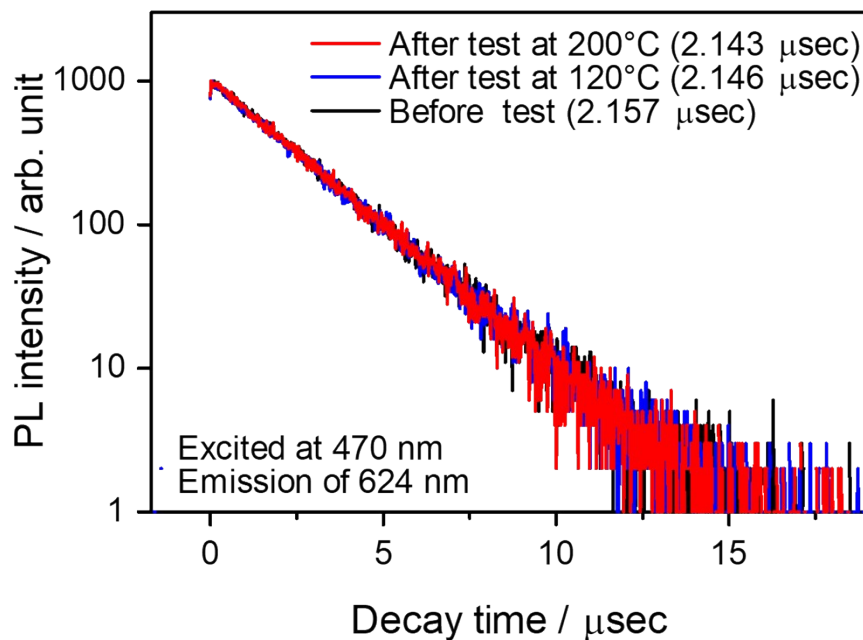


Figure S12 PL decay curves for the NMP:_{0.030}Eu²⁺-MPQ phosphors before and after the humidity test.